

Tetranuclear Nickel(II) Complexes Composed of Pairs of Dinuclear LNi_2 Fragments Linked by Acetylenedicarboxylate, Terephthalate, and Isophthalate Dianions: Synthesis, Structures and Magnetic Properties

Julia Klingele,^[a] Marco H. Klingele,^{[a]†} Oliver Baars,^[b] Vasile Lozan,^[b] Axel Buchholz,^[c] Guido Leibelng,^[d] Winfried Plass,^[c] Franc Meyer,^[d] and Berthold Kersting^{*[b]}

Keywords: Macrocyclic ligands / Dicarboxylate ligands / Nickel / Polynuclear complexes / Magnetic properties

The tetranuclear nickel(II) complexes $[(\text{LNi}^{\text{II}})_2(\text{acetylenedicarboxylate})][\text{BPh}_4]_2$ (**2**), $[(\text{LNi}^{\text{II}})_2(\text{terephthalate})][\text{BPh}_4]_2$ (**3**), and $[(\text{LNi}^{\text{II}})_2(\text{isophthalate})][\text{BPh}_4]_2$ (**4**), where L^{2-} represents a macrocyclic hexaaza-dithiophenolate ligand, have been synthesized and characterized by UV/Vis spectroscopy, IR spectroscopy, X-ray crystallography, and magnetic susceptibility measurements. Each dicarboxylate dianion acts as a quadridentate bridging ligand linking two bioctahedral LNi_2 units via $\mu_{1,3}$ -bridging carboxylate functions to generate discrete $[(\text{LNi}^{\text{II}})_2(\text{dicarboxylate})]^{2+}$ dications with a central $\text{LNi}_2(\text{O}_2\text{C}-\text{R}-\text{CO}_2)\text{Ni}_2\text{L}$ core. The structures differ mainly in the distance between the center of the $\text{Ni}\cdots\text{Ni}$ axes of the isostructural LNi_2 units (8.841(1) Å in **2**, 10.712(1) in **3**, and 9.561(1) in

4). The tilting angle between the two Ni_2O_2 planes (86.3° in **2**, 58.2° in **3**, 20.9° in **4**). Magnetic susceptibility measurements on the complexes over the range 2.0–295 K reveal the presence of weak ferromagnetic exchange interactions between the Ni^{II} ions within the dinuclear subunits with values for the magnetic exchange constant J_1 of 23.1(5), 18.1(5), and 14.2(5) cm^{-1} for **2**, **3**, and **4**, respectively ($\mathbf{H} = -2J_1\mathbf{S}_1\mathbf{S}_2$). The magnitude of the exchange interaction J_2 across the dicarboxylate bridges is in all cases less than 0.1 cm^{-1} , suggesting that no significant interdimer exchange coupling occurs in **2**–**4**.

(© Wiley-VCH Verlag GmbH & Co. KGaA, 69451 Weinheim, Germany, 2007)

Introduction

The carboxylate group, RCO_2^- , can bind to transition metals in a variety of coordination modes giving rise to complexes of great structural diversity.^[1] Current activities focus on the coordination chemistry of polycarboxylate ligands, as these offer great potential in the construction of polynuclear aggregates^[2] and extended coordination polymers with micro- and mesoporous structures^[3–6] or catalytic properties.^[7] In addition, polycarboxylate ligands are of importance as spin-coupling bridging ligands^[8–15] in the rapidly expanding field of molecular magnetism.^[16,17] In

this context, an enormous amount of literature has been generated concerning the distance dependence of magnetic exchange interactions between metal atoms linked by extended dicarboxylate ligands. Dinuclear copper complexes bridged by oxalate^[18,19] and terephthalate^[20–22] dianions form, by far, the largest group of such systems, and it appears that the exchange interactions depend on the $\text{M}\cdots\text{M}$ distance,^[23] the relative orientation of the magnetic orbitals,^[24] and the degree of conjugation of the organic spacer unit.^[25,26]

Recently, we reported the structures and magnetic properties of an isostructural series of bioctahedral $[\text{LM}^{\text{II}}_2(\text{OAc})]^+$ complexes, where L^{2-} represents a macrodinucleating N_6S_2 supporting ligand (Scheme 1).^[27] Intramolecular antiferromagnetic exchange interactions are present in the Mn^{II}_2 , Fe^{II}_2 and Co^{II}_2 complexes of this series with J values of -5.1 , -10.6 , and -2.0 cm^{-1} ($\mathbf{H} = -2J_1\mathbf{S}_1\mathbf{S}_2$). In contrast, in the corresponding Ni^{II}_2 complex a ferromagnetic exchange interaction is present with $J = +6.4$ cm^{-1} .

In view of the increasing interest in the targeted assembly of molecular-based magnetic materials using high-spin molecules of higher nuclearity,^[28–34] we considered it worthwhile to examine the possibility of linking pairs of dinuclear $[\text{LNi}^{\text{II}}_2]$ units by dicarboxylate dianions to form tetranuclear species. In the present contribution we report the synthesis and crystallographic characterization of three novel

[a] Institut für Anorganische und Analytische Chemie, Universität Freiburg, Albertstr. 21, 79104 Freiburg, Germany

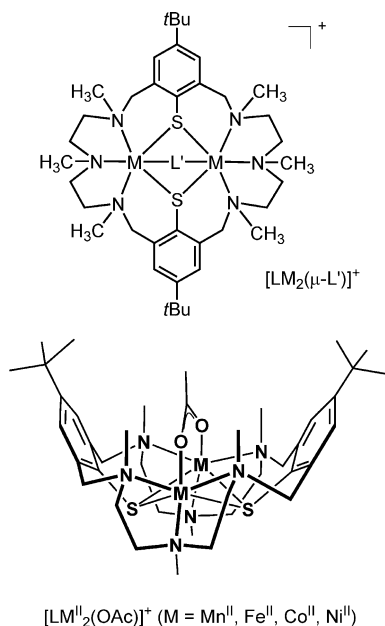
[b] Institut für Anorganische Chemie, Universität Leipzig, Johannisallee 29, 04103 Leipzig, Germany
Fax: +49-341-973-6199
E-mail: b.kersting@uni-leipzig.de

[c] Institut für Anorganische Chemie und Analytische Chemie, Universität Jena, Carl-Zeiss-Promenade 10, 07745 Jena, Germany

[d] Institut für Anorganische Chemie, Georg-August-Universität Göttingen, Tammannstrasse 4, 37077 Göttingen, Germany

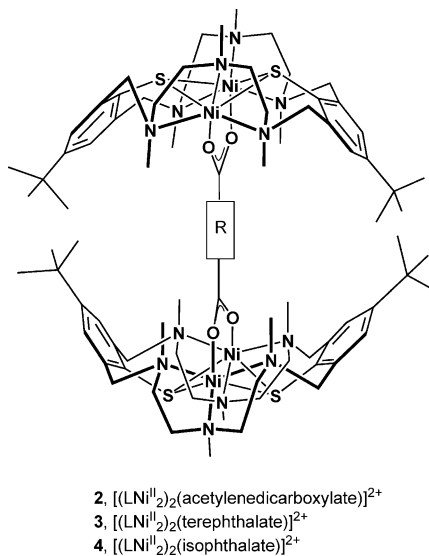
[†] Present address: IoLiTec Ionic Liquids Technologies GmbH & Co. KG, Ferdinand-Porsche-Str. 5/1, 79211 Denzlingen, Germany

Supporting information for this article is available on the WWW under <http://www.eurjic.org> or from the author.



Scheme 1. Dinuclear acetate-bridged complexes of the hexaaza-dithiophenolate ligand L^{2-} .

tetranuclear nickel(II) complexes of the type $[\text{LNi}^{\text{II}}_2\text{dicarboxylateNi}^{\text{II}}_2\text{L}]$, where “dicarboxylate” stands for acetylenedicarboxylate, terephthalate, or isophthalate dianions. A schematic representation of these complexes is shown in Scheme 2. These novel complexes differ by the distance between the centre of the $\text{Ni}\cdots\text{Ni}$ axis of the isostructural LNi_2 subunits, their relative orientation, and the nature of the bridging ligands. The ability of the dicarboxylate dianions to mediate magnetic exchange interactions between the dinuclear subunits is examined and discussed in the light of their specific structural features.

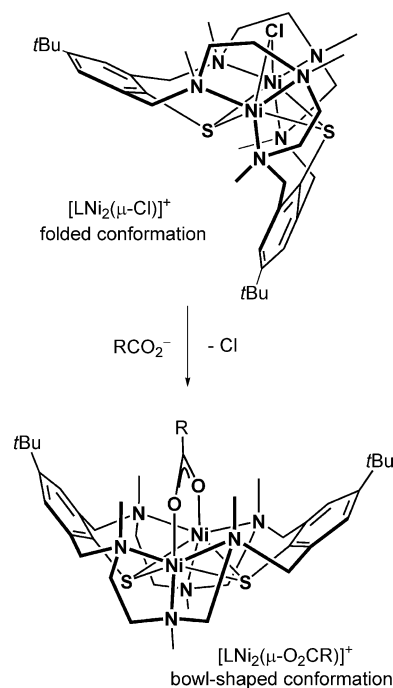


Scheme 2. Complexes prepared and their labels.

Synthesis and Characterization of the Complexes

The complexes $[(\text{LNi}^{\text{II}}_2)_2(\text{acetylenedicarboxylate})]^{2+}$ (**2**), $[(\text{LNi}^{\text{II}}_2)_2(\text{terephthalate})]^{2+}$ (**3**), and $[(\text{LNi}^{\text{II}}_2)_2(\text{isophthalate})]^{2+}$

(**4**) were readily prepared from the reaction of the dinuclear complex $[\text{LNi}^{\text{II}}_2(\mu\text{-Cl})]^+$ (**1**) and the corresponding triethylammonium dicarboxylate, prepared in situ from the acid and triethylamine in methanol in a 1:2 molar ratio, and isolated in high yield as the perchlorate or tetraphenylborate salts. The transformations are not simple substitution reactions, because simultaneous conformational changes of the supporting ligand L^{2-} from the folded (C_3 -symmetric) to the “bowl-shaped” (C_{2v} -symmetric) conformation take place (see Scheme 3).^[35] Nonetheless, linking of two $[\text{LNi}_2]^{2+}$ fragments by the carboxylato ligands is a clean and facile step driven by the low solubility of the products.



Scheme 3. Schematic representation of the two ligand conformations in the chloro- and carboxylato-bridged complexes of $(\text{L})^{2-}$. For these conformational changes metal–ligand dissociations are required.

All compounds gave satisfactory elemental analyses and their IR spectra are marked by the prominent asymmetric and symmetric carboxylate stretching frequencies around 1580 cm^{-1} and 1420 cm^{-1} , diagnostic of $\mu_{1,3}$ -bridging carboxylate functions.^[36] The UV/Vis spectra of **2–4** in acetonitrile display two weak bands above 500 nm typical of octahedral Ni^{2+} (d^8 , $S = 1$) ions. The observed values compare closely with those of the acetato-bridged complex $[\text{LNi}^{\text{II}}_2(\text{OAc})]^+$,^[27] indicative of a pseudo-octahedral $\text{N}_3\text{S}_2\text{O}$ coordination environment about the metal ions. This is confirmed by single-crystal X-ray crystallography.

Description of the Crystal Structures

Crystals of $2[\text{BPh}_4]_2 \cdot 2\text{MeCN} \cdot 0.5\text{H}_2\text{O}$ were obtained by slow evaporation of an acetonitrile/ethanol (1:1) solution of **2** $[\text{BPh}_4]_2$. The crystal structure is composed of tetranuclear $[(\text{LNi}^{\text{II}}_2)_2(\text{acetylenedicarboxylate})]^{2+}$ dications, tetraphen-

ylborate anions and acetonitrile and water solvates. Perspective drawings of the structure of **2** are depicted in Figure 1. Selected bond lengths and angles are summarized in Table 1.

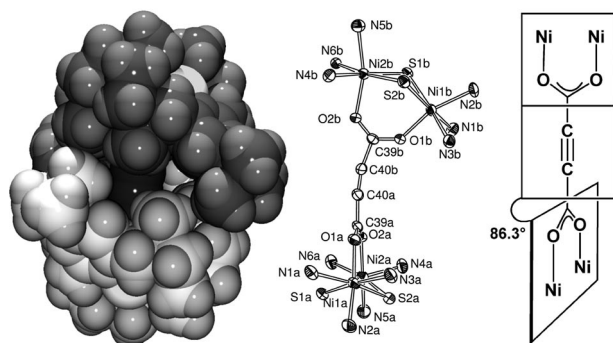


Figure 1. Left: van der Waals plot of the $[(\text{LNi}^{\text{II}})_2(\text{acetylenedicarboxylato})]^{2+}$ dication in crystals of $2[\text{BPh}_4]_2 \cdot \text{MeCN} \cdot 0.5\text{H}_2\text{O}$. Middle: ORTEP representation of the core structure of **2** with the atom labeling scheme. Ellipsoids are represented at the 50% probability level. Right: Mutual orientation of the Ni_2 carboxylato planes in **2**.

The acetylenedicarboxylate dianion acts as a tetradentate bridging ligand joining two dinuclear $[\text{LNi}^{\text{II}}_2]^{2+}$ fragments through its carboxylate functions to give a tetranuclear $\text{Ni}_2(\text{O}_2\text{CC}\equiv\text{CCO}_2)\text{Ni}_2$ array. Each nickel atom is surrounded in a highly distorted octahedral fashion by two sulfur atoms and three nitrogen atoms from the supporting ligand, and one oxygen atom from the acetylenedicarboxylate moiety. The Ni_2 carboxylato planes are necessarily twisted by 86.3° about the $\text{C}\equiv\text{C}$ bond to relieve the unfavourable steric interactions between the bulky *t*Bu groups of the two opposing $[\text{LNi}^{\text{II}}_2]^{2+}$ subunits. The coligand is also slightly bent ($\text{C}\equiv\text{C}$ 1.185(6) Å) such that the intramolecular distances between two nickel atoms of different dinuclear subunits within the tetranuclear complex range from 8.623(1) to 9.769(1) Å. The only system comparable to that of **2** is provided by the complex $[\{\text{Mo}_2(\text{DAniF})_3\}_2(\text{O}_2\text{CC}\equiv\text{CCO}_2)]$, where $\text{DAniF} = N,N'$ -di-*p*-anisylformamidinate, for which an intramolecular $\text{Mo}\cdots\text{Mo}$ distance of 9.537 Å has been reported.^[37] There are no significant intermolecular interactions between the Ni^{II}_4 complexes within the lattice. The shortest intermolecular $\text{Ni}\cdots\text{Ni}$ distance is at 7.470(1) Å.

Table 1. Selected bond lengths [Å] and angles [°] in **2–4**.

	$2[\text{BPh}_4]_2 \cdot \text{MeCN} \cdot \text{H}_2\text{O}^{[\text{a}]}$	$3[\text{BPh}_4]_2 \cdot 2\text{EtOH} \cdot \text{MeCN}_{0.5} \cdot \text{H}_2\text{O}^{[\text{a}]}$	$4[\text{BPh}_4]_2 \cdot 4\text{MeCN} \cdot \text{EtOH}^{[\text{a}]}$
Ni(1a)–O(1a)	2.017(3) [1.974(3)]	1.992(3) [1.995(3)]	2.044(1) [1.989(2)]
Ni(1a)–N(1a)	2.302(5) [2.306(4)]	2.347(4) [2.286(4)]	2.312(2) [2.309(2)]
Ni(1a)–N(2a)	2.160(4) [2.133(4)]	2.141(4) [2.135(4)]	2.157(2) [2.133(2)]
Ni(1a)–N(3a)	2.212(4) [2.277(4)]	2.199(4) [2.228(4)]	2.228(2) [2.255(2)]
Ni(1a)–S(1a)	2.504(2) [2.486(2)]	2.457(2) [2.507(2)]	2.4750(7) [2.4981(6)]
Ni(1a)–S(2a)	2.399(2) [2.408(2)]	2.469(2) [2.486(2)]	2.4418(6) [2.4311(6)]
Ni(2a)–O(2a)	2.028(3) [2.078(3)]	2.002(3) [2.007(3)]	1.998(1) [2.032(1)]
Ni(2a)–N(4a)	2.226(5) [2.189(4)]	2.266(4) [2.246(4)]	2.215(2) [2.204(2)]
Ni(2a)–N(5a)	2.159(5) [2.190(4)]	2.147(4) [2.157(4)]	2.155(2) [2.146(2)]
Ni(2a)–N(6a)	2.296(5) [2.279(4)]	2.242(4) [2.280(4)]	2.281(2) [2.346(2)]
Ni(2a)–S(1a)	2.503(2) [2.497(2)]	2.504(2) [2.489(2)]	2.5099(6) [2.4567(7)]
Ni(2a)–S(2a)	2.398(2) [2.446(2)]	2.451(2) [2.460(2)]	2.4317(6) [2.4523(6)]
N–O	2.024(3)	1.999(3)	2.016(1)
Ni–N	2.227(5)	2.223(4)	2.228(2)
Ni–S	2.455(2)	2.478(2)	2.4621(6)
C(39a)–O(1a)	1.261(6) [1.258(5)]	1.257(5) [1.257(5)]	1.255(2) [1.258(2)]
C(39a)–O(2a)	1.250(6) [1.245(6)]	1.265(5) [1.260(5)]	1.265(2) [1.263(2)]
Ni(1a)⋯Ni(2a)	3.469(1)	3.460(1)	3.475(1)
Ni(1b)⋯Ni(2b)	3.486(1)	3.507(1)	3.459(1)
Ni(1a)⋯Ni(1b)	8.623(1)	11.028(1)	8.120(1)
Ni(1a)⋯Ni(2b)	9.508(1)	10.947(1)	10.122(1)
Ni(2a)⋯Ni(1b)	8.757(1)	10.833(1)	9.909(1)
Ni(2a)⋯Ni(2b)	9.769(1)	11.155(1)	11.097(1)
Ni–Ni ^{cent} /Ni–Ni ^{cent} [b]	8.841(1)	10.712(1)	9.561(1)
O–M–N ^{cis} [c]	87.7(2) [87.3(2)]	88.7(2) [88.2(2)]	88.26(6) [88.12(6)]
O–M–N ^{trans} [c]	162.3(2) [162.6(2)]	164.8(2) [164.9(2)]	164.27(6) [164.13(6)]
S–M–N ^{cis} [c]	94.5(2) [94.7(1)]	93.8(1) [94.2(1)]	94.00(5) [93.94(5)]
S–M–N ^{trans} [c]	168.9(1) [169.0(1)]	170.5(1) [169.8(1)]	169.52(5) [169.73(5)]
S–M–S[c]	78.91(6) [78.82(5)]	80.4(1) [79.25(5)]	79.47(2) [79.92(2)]
S–M–O[c]	94.6(1) [94.4(1)]	94.3(1) [94.1(1)]	94.52(4) [94.49(4)]
N–M–N[c]	87.8(2) [87.9(2)]	87.6(2) [87.8(2)]	87.61(6) [87.66(7)]
M–S–M[c]	90.18(6) [90.31(5)]	88.91(5) [89.76(5)]	89.30(2) [89.76(6)]
$\text{RCO}_2/\text{RCO}_2^{[\text{d}]}$	86.3	58.2	20.9
$\text{RCO}_2/\text{Ph}^{[\text{e}]}$	–	39.1 [19.1]	9.6 [12.8]

[a] Numbers in square brackets correspond to atoms labeled “b”. [b] Distance between center of the $\text{Ni}\cdots\text{Ni}$ axes of the Ni_2 units. [c] Average values. [d] Angle between the normals of the planes of the carboxylate functions. [e] Twist angle of the carboxylato planes with respect to the aromatic ring of the dicarboxylate dianion.

Figure 2 shows the structure of the tetranuclear nickel(II) complex **3** in crystals of $3[\text{BPh}_4]_2 \cdot 2\text{EtOH} \cdot 0.5\text{MeCN} \cdot \text{H}_2\text{O}$. Again, the terephthalato ligand acts as a bifunctional linker coordinating to two bioctahedral $[\text{LNi}^{\text{II}}_2]^{2+}$ entities via the carboxylate functions to generate a twisted $\text{Ni}_2\text{O}_2\text{C}-\text{C}_6\text{H}_4-\text{CO}_2\text{Ni}_2$ motif.

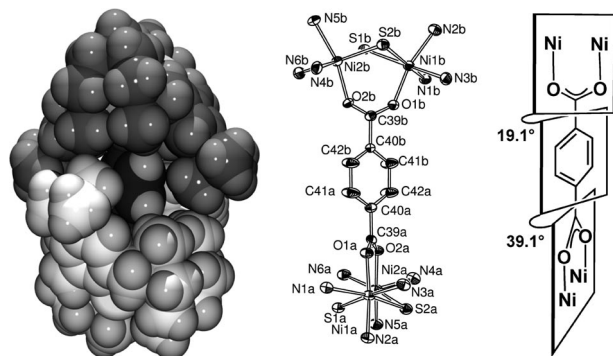


Figure 2. Left: van der Waals representation of the $[(\text{LNi}^{\text{II}}_2)_2(\mu\text{-terephthalato})]^{2+}$ dication in crystals of $3[\text{BPh}_4]_2 \cdot 2\text{EtOH} \cdot 0.5\text{MeCN} \cdot \text{H}_2\text{O}$. Middle: ORTEP representation of the core structure of **3** with the atom labeling Scheme. Ellipsoids are represented at the 50% probability level. Right: Relative orientation of the Ni_2 -carboxylato planes in **3**.

The $[\text{LNi}_2]^{2+}$ subunits in **2** and **3** are structurally very similar, and the Ni–N, Ni–O, and Ni–S distances lie within very narrow ranges (Table 1). As in **2**, the *t*Bu groups of the two opposing Ni_2 clusters are forced to interlock to accommodate the terephthalato ligand. This causes tilting of the carboxylato planes that are rotated by 58.2° with respect to each other and by 19.1° and 39.1° with respect to the aromatic ring of the terephthalato coligand. Again, there are no intermolecular interactions between the tetranuclear complexes other than van der Waals contacts. The intramolecular Ni \cdots Ni distances between the two dinuclear subunits are within the range 10.833(1)–11.155(1) Å (mean 10.990(1) Å). This is a typical value for terephthalato-bridged nickel(II) complexes.^[38,39]

Crystals of $4[\text{BPh}_4]_2 \cdot 4\text{MeCN} \cdot \text{EtOH}$ are triclinic, space group $P\bar{1}$. ORTEP views of the structure of the dication **4** and the central core are provided in Figure 3. Selected bond lengths and angles are given in Table 1.

The isophthalate dianion is bonded to two $[\text{LNi}^{\text{II}}_2]^{2+}$ units through $\mu_{1,3}$ -bridging carboxylate functions. The metal–ligand bond lengths within **4** reveal no anomalies and are very similar to those in **2** and **3** (Table 1). Strangely, the twisting of the carboxylato planes is less pronounced than in the previous cases. In fact, the two planes are almost coplanar with the phenyl ring of the bridging isophthalate dianion. The geometrical requirements of the isophthalate moiety with the two carboxylate functions in *meta* orientation leads to a distance of 9.561 Å between the center of the Ni \cdots Ni axes of the dinuclear units. This value should be compared with that of 10.712 Å in **3**, where the two carboxylate functions are in *para* positions. The present coordination mode of the isophthalate dianion forming a discrete Ni^{II}_4 cluster is without precedence in the literature.^[40–42]

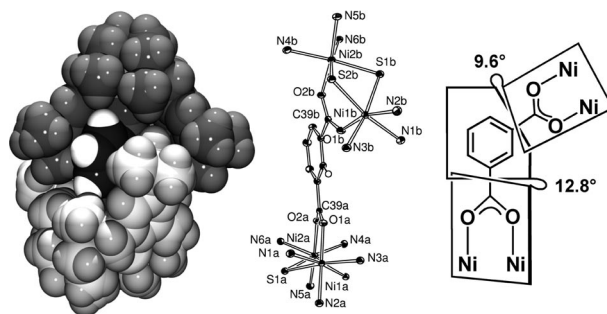


Figure 3. Left: van der Waals representation of the $[(\text{LNi}^{\text{II}}_2)_2(\mu\text{-isophthalato})]^{2+}$ dication in crystals of $4[\text{BPh}_4]_2 \cdot 4\text{MeCN} \cdot \text{EtOH}$. Middle: ORTEP representation of the core structure of **4** with the atom labeling Scheme. Ellipsoids are represented at the 50% probability level. Right: Tilting of the Ni_2 -carboxylato planes in **4**.

In summary, all three new compounds are discrete tetranuclear nickel(II) complexes composed of pairs of bioctahedral $[\text{LNi}^{\text{II}}_2]^{2+}$ units united by a tetradentate dicarboxylate anion. The calixarene-like conformation adopted by the supporting ligand leads to an almost complete encapsulation of the $\text{Ni}_2(\text{O}_2\text{C}-\text{R}-\text{CO}_2)\text{Ni}_2$ core. As a consequence the Ni^{II}_4 clusters are well-separated from each other in the solid state, featuring only intermolecular van der Waals contacts. This aspect of the structures will be relevant in the following discussion of the magnetic properties of the complexes.

Magnetic Properties

The magnetic properties of the three carboxylato-bridged complexes were examined in view of literature reports that conjugated dicarboxylate ligands are able to mediate long-range magnetic exchange interactions between paramagnetic metal ions.^[43] The variable-temperature magnetic susceptibility data for **2** $[\text{BPh}_4]_2$, **3** $[\text{BPh}_4]_2$, and **4** $[\text{BPh}_4]_2$ were measured over the range 2.0–295 K using a SQUID magnetometer and an applied external magnetic field of 0.2 T. Plots of the temperature dependence of the effective magnetic moment μ_{eff} for the three compounds are shown in Figure 4. The complexes have similar magnetic properties. At room temperature, the respective values of μ_{eff} are 6.91 μ_{B} , 6.82 μ_{B} , and 7.13 μ_{B} per tetranuclear complex. With decreasing temperature the μ_{eff} values increase steadily to maximum values of 7.85 μ_{B} (15 K), 7.71 μ_{B} (15 K), and 8.03 μ_{B} (25 K) for **2** $[\text{BPh}_4]_2$, **3** $[\text{BPh}_4]_2$, and **4** $[\text{BPh}_4]_2$, respectively. On lowering the temperature to 2.0 K, these values decrease slightly down to 7.57 μ_{B} , 7.02 μ_{B} , and 5.78 μ_{B} at 2 K, presumably due to saturation effects or the zero-field splitting of nickel(II).

In all cases the maximum value of the effective magnetic moment is lower than expected for a spin-only value of 9.84 μ_{B} for $S_{\text{T}} = 4$ resulting from ferromagnetic coupling of four Ni^{II} ($S_i = 1$, $g = 2.20$) ions. However, the values are also significantly larger than the value of 6.22 μ_{B} calculated for completely uncoupled spins. The overall behaviour indi-

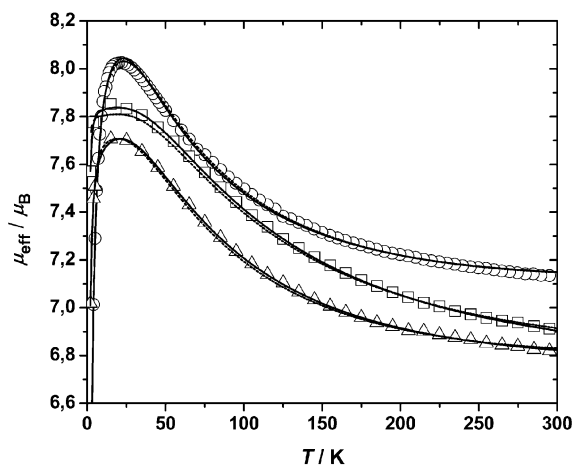


Figure 4. Temperature dependence of μ_{eff} (per tetranuclear complex) for $2[\text{BPh}_4]_2$ (open squares), $3[\text{BPh}_4]_2$ (open triangles), and $4[\text{BPh}_4]_2$ (open circles). The full lines represent the best theoretical fits to Equation (1). The dashed lines represent the best fits to the dimer model in Equation (3). Experimental and calculated values are provided in the electronic supporting information.

icates the presence of weak ferromagnetic exchange interactions between the Ni^{2+} ions within the dinuclear subunits, but negligible, if any, coupling across the dicarboxylate bridges. The latter behaviour can be attributed to the long distance between the Ni^{2+} ions spanned by the dicarboxylates. In this regard, it is worth noting that very weak exchange interactions have indeed been reported for other terephthalato- or isophthalato-bridged nickel(II) complexes.^[26,44,45]

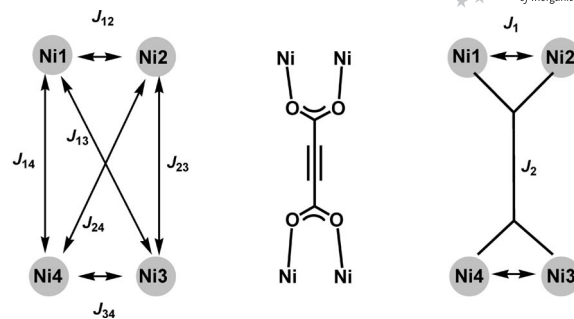
In order to determine the magnitude of the exchange interactions, the magnetic susceptibility data were simulated by using Equation (1), where χ_{tetra} and χ_{mono} refer to the molar susceptibilities of a Ni_4 complex and a fraction ρ of a mononuclear nickel(II) impurity with Curie constant $C = Ng^2\mu_{\text{B}}^2/3kT$.

$$\chi = \chi_{\text{tetra}}(1-\rho) + 4\chi_{\text{mono}}\rho \quad (1)$$

The molar magnetic susceptibility χ_{tetra} was derived from the appropriate spin-Hamiltonian [Equation (2)] including the isotropic Heisenberg exchange, the single-ion zero-field splitting and the single-ion Zeeman interaction by a full-matrix diagonalization approach.^[34]

$$H = -2J_1(\hat{S}_1 \cdot \hat{S}_2 + \hat{S}_3 \cdot \hat{S}_4) - 2J_2(\hat{S}_1 \cdot \hat{S}_3 + \hat{S}_1 \cdot \hat{S}_4 + \hat{S}_2 \cdot \hat{S}_3 + \hat{S}_2 \cdot \hat{S}_4) \\ H = H_{\text{ex}} + \sum_{i=1}^4 [D_i(\hat{S}_i^2 - \frac{1}{3}S_i(S_i+1)) + g_i\mu_{\text{B}}B_z\hat{S}_{iz}] \quad (\tau = x, y, z) \quad (2)$$

In this model J_1 ($= J_{12} = J_{34}$) represents the exchange interaction between the Ni^{2+} ions within the dinuclear subunit, whereas J_2 ($J_{13} = J_{14} = J_{23} = J_{24}$) describes the interaction across the dicarboxylate linker. In order to reduce the number of variables, the D and g values were considered to be identical for all of the four Ni^{2+} ions.



The least-squares fitting of the experimental data over the full temperature range led to $J_1 = +23.1(5) \text{ cm}^{-1}$, $J_2 = -0.0045(10) \text{ cm}^{-1}$, $g = 2.27(1)$, $D = -1.9(5) \text{ cm}^{-1}$, $\rho = 0.010(5)\%$ for $2[\text{BPh}_4]_2$, $J_1 = +18.1(5) \text{ cm}^{-1}$, $J_2 = -0.0048(9) \text{ cm}^{-1}$, $g = 2.24(1)$, $D = -1.5(5) \text{ cm}^{-1}$, $\rho = 0.020(5)\%$ for $3[\text{BPh}_4]_2$, and $J_1 = +14.2(5) \text{ cm}^{-1}$, $J_2 = -0.071(9) \text{ cm}^{-1}$, $g = 2.37(1)$, $D = 9.6(5) \text{ cm}^{-1}$, $\rho = 0.020(5)\%$ for $4[\text{BPh}_4]$. The inclusion of the D parameter improves the low-temperature fit significantly, but it represents by no means an accurate value since temperature-dependent magnetic susceptibility measurements are not very appropriate for the determination of D .^[46,47] The experimentally determined J_2 parameters are very small and should be taken as indicative rather than definite, because they are beyond the detection limit of the technique. Nevertheless, it is clear that magnetic exchange interactions via the dicarboxylate linkers are not significant (estimated upper limit for J_2 : $\pm 0.1 \text{ cm}^{-1}$) and that the magnetic properties of the tetranuclear systems are solely based on the exchange couplings in the binuclear $[\text{LNi}_2(\text{O}_2\text{CR})]^+$ subunits. In this respect, we also tried to simulate the temperature dependence of the magnetic data by using an isotropic dimer model [Equation (3)] for two Ni^{II} ($S = 1$) ions based on the Hamiltonian in Equation (4).

$$\chi = 2[\chi_{\text{dim}}(1-\rho) + 2\chi_{\text{mono}}\rho] \quad (3)$$

$$H = -2JS_xS_z + \sum_{i=1}^2 [D_i(\hat{S}_i^2 - \frac{1}{3}S_i(S_i+1)) + g_i\mu_{\text{B}}B_z\hat{S}_{iz}] \quad (\tau = x, y, z) \quad (4)$$

The magnetic data could be reproduced equally well by this approach (Figure 4), yielding $J_1 = +23.4(5) \text{ cm}^{-1}$, $g = 2.26(1)$, $D = -2.2(5) \text{ cm}^{-1}$, $\rho = 0.010\%$ for $2[\text{BPh}_4]_2$, $J_1 = +19.3(4) \text{ cm}^{-1}$, $g = 2.23(1)$, $D = -4.8(5) \text{ cm}^{-1}$, $\rho = 0.035\%$ for $3[\text{BPh}_4]_2$, and $J_1 = +15.5(5) \text{ cm}^{-1}$, $g = 2.35$, $D = 12.0(5) \text{ cm}^{-1}$, $\rho = 0.03\%$ for $4[\text{BPh}_4]$. Again, this analysis establishes a weak ferromagnetic coupling between the two Ni^{II} ions. All of these values are in excellent agreement with those reported for the dinuclear nickel(II) complexes $[\text{LNi}^{\text{II}}_2(\text{OAc})][\text{BPh}_4]$ and $[\text{LNi}^{\text{II}}_2(\text{OBz})][\text{BPh}_4]$,^[48] providing further support for the absence of significant interdimer exchange coupling in $2[\text{BPh}_4]_2$ – $4[\text{BPh}_4]_2$.

There has been much interest in the distance-dependence of superexchange interactions between paramagnetic transition metal ions bridged by extended organic spacer ligands.^[22,23] In this regard a large number of dicarboxylato-bridged copper(II) dimers with $\text{Cu}\cdots\text{Cu}$ separations of 5 to 15 Å have been prepared and their magnetic properties have

been determined.^[22,23] In general, the magnetic exchange interactions decrease rapidly with increasing M···M separations and the experimentally determined J values approach the values predicted by the Coffman Buettner relation ($|J| \leq 1 \text{ cm}^{-1}$ for $d(\text{M} \cdots \text{M}) \geq 9 \text{ \AA}$).^[23,49] Cano et al. have shown that this finding also applies to other paramagnetic metal ions,^[26] and the *interdimer* exchange couplings of the present complexes ($|J| \leq 0.1 \text{ cm}^{-1}$, $d(\text{Ni}_2 \cdots \text{Ni}_2) 8.623\text{--}11.155 \text{ \AA}$) are in good agreement with the reported trend. There seems to be no dependence of the *interdimer* coupling on the mutual orientation of the Ni_2O_2 planes, which is in line with our previous observations.^[50]

Conclusions

In summary, we presented the synthesis and characterization of the first members of a new class of tetranuclear nickel(II) complexes in which pairs of dinuclear Ni_2 -aminethiophenolate complexes are linked by acetylenedicarboxylate, terephthalate and isophthalate groups. The complexes are readily prepared and exist as stable and discrete complexes in solution and in the solid state as ascertained by various spectroscopic methods and X-ray crystallography. The magnetic properties of these compounds reveal the presence of weak ferromagnetic exchange interactions between the Ni^{II} ions of the dinuclear subunits and negligible coupling across the dicarboxylate bridges. A dependence of the *interdimer* coupling on the mutual orientation of the Ni_2O_2 planes was not observed. High-spin molecules of this sort are presumably only accessible with shorter bridging ligands such as oxalate or squarate dianions. These studies are underway.

Experimental Section

General Remarks: Solvents and reagents were of reagent grade quality and used as received unless otherwise specified. $[\text{LNi}^{\text{II}}_2(\mu\text{-Cl})\text{ClO}_4]$ was prepared according to a literature procedure.^[51] Melting points were determined in open glass capillaries and are uncorrected. IR spectra were measured on a Bruker VECTOR 22 FT-IR spectrophotometer as KBr pellets, electronic absorption spectra on a Jasco V-570 UV/Vis/Near IR spectrophotometer. Temperature-dependent magnetic susceptibility measurements on powdered solid samples were carried out on a SQUID magnetometer (MPMS Quantum Design) over the temperature range 2.0–295 K. The measurements were performed at applied magnetic fields of 0.20 and 0.50 T. For all three compounds, the magnetic behaviour does not change with field. The observed susceptibility data were corrected for underlying diamagnetism using Pascal's constants.

Derivation of the Magnetic Susceptibility Expression for Tetranuclear Ni Complexes: The complete matrix of H can be calculated by writing out the coupled states and determining the matrix elements by elementary operations with angular momenta operators.^[52,53] The resulting Hamiltonian matrix is diagonalized numerically for given values of J_1 , J_2 , g and D . The slope of E vs. B is calculated at the desired field; this slope is the magnetic moment for the i^{th} energy level. The molar paramagnetic susceptibility, χ , of the system is then calculated as a function of temperature using Equation (1), where χ_{tetra} and χ_{mono} refer to the molar susceptibilities

of the tetranuclear complex [Equation (5)] and the fraction ρ of a mononuclear nickel(II) impurity with Curie constant $C = Ng^2\mu_B^2/3kT$ [Equation (6)]. χ_{dim} is the molar susceptibility of the binuclear subunit. A least-squares program then compares calculated and observed susceptibility curves and changes the parameters to get the best fit.^[34]

$$\chi_{\text{tetra}} = \frac{N \sum_i (-\partial E_i / \partial B) \exp(-E_i / kT)}{\sum_i \exp(-E_i / kT)} \quad (5)$$

$$\chi_{\text{mono}} = \frac{Ng^2\mu_B^2}{3kT} \left(\frac{2}{2} + 1 \right) \quad (6)$$

Safety note! Caution: Perchlorate salts of transition metal complexes are hazardous and may explode. Only small quantities should be prepared and handled with great care.

$[\text{LNi}^{\text{II}}_2(\text{acetylenedicarboxylato})][\text{ClO}_4]_2$ ($2[\text{ClO}_4]_2$): Triethylamine (50 mg, 0.50 mmol) was added to a solution of acetylenedicarboxylic acid (28.5 mg, 0.250 mmol) in methanol (30 mL). $[\text{LNi}^{\text{II}}_2\text{Cl}][\text{ClO}_4]$ ($1[\text{ClO}_4]$) (461 mg, 0.500 mmol) was added to this solution with constant stirring. A green precipitate resulted immediately. Additional $\text{LiClO}_4 \cdot 3\text{H}_2\text{O}$ (160 mg, 1.00 mmol) was added to ensure complete precipitation of the product. After stirring for 1 d, the green precipitate was collected by filtration, washed several times with cold methanol and dried in the air. Yield 335 mg (71%), m.p. 302–303 °C (decomp.). IR (KBr): $\tilde{\nu} = 3439$ (m), 2963 (s), 2869 (s), 2249 (w), 2018 (w), 1596 [s, $\nu_{\text{asym}}(\text{RCO}_2^-)$], 1463 (s), 1424 (w), 1394 [w, $\nu_{\text{sym}}(\text{RCO}_2^-)$], 1355 (s), 1264 (m), 1235 (m), 1202 (w), 1170 (w), 1154 (m), 1096 [vs, $\nu_3(\text{ClO}_4^-)$], 1039 (s), 1001 (w), 984 (w), 932 (m), 912 (m), 881 (m), 826 (s), 819 (m), 809 (m), 766 (w), 754 (w), 682 (m), 624 [vs, $\nu_4(\text{ClO}_4^-)$] (s), 602 (w), 564 (w), 545 (w), 535 (w), 493 (w), 441 (w), 417 cm^{-1} (w).

$[\text{LNi}^{\text{II}}_2(\text{acetylenedicarboxylato})][\text{BPh}_4]_2$ ($2[\text{BPh}_4]_2$): A solution of NaBPh_4 (342 mg, 1.00 mmol) in ethanol (50 mL) was added to a solution of $2[\text{ClO}_4]_2$ (188 mg, 0.100 mmol) in acetonitrile (150 mL). The reaction mixture was allowed to stir for 1 h, before the volume of the solution was reduced in vacuo to about 50 mL. The green product was filtered, washed with ethanol and dried in the air to give 190 mg (82%) of $2[\text{BPh}_4]_2$ as a green, air-stable, microcrystalline powder, m.p. 279–280 °C (decomp.). IR (KBr (cm^{-1})): $\tilde{\nu} = 3434$ (s), 3122 (w), 3054 (s), 3030 (s), 2963 (s), 2867 (s), 2808 (m), 1945 (w), 1880 (w), 1815 (w), 1763 (w), 1597 [s, $\nu_{\text{asym}}(\text{CO}_2^-)$], 1461 (s), 1425 (m), 1392 [m, $\nu_{\text{sym}}(\text{CO}_2^-)$], 1355 (s), 1308 (m), 1264 (m), 1235 (m), 1202 (w), 1170 (w), 1154 (m), 1133 (w), 1078 (s), 1058 (s), 1039 (s), 999 (w), 930 (w), 911 (w), 882 (w), 824 (m), 733 [s, $\nu(\text{BPh}_4^-)$], 705 [s, $\nu(\text{BPh}_4^-)$], 681 (m), 627 (m), 612 (m), 563 (w), 544 (w), 492 (w), 470 (w), 414 (w). UV/Vis (CH_2Cl_2): λ_{max} (ϵ) = 656 (32), 1091 nm ($82 \text{ M}^{-1} \text{ cm}^{-1}$). $\text{C}_{128}\text{H}_{168}\text{B}_2\text{N}_{12}\text{Ni}_4\text{O}_4\text{S}_4$ (2323.44): calcd. C 66.17, H 7.29, N 7.23, S 5.52; found C 65.85, H 7.31, N 7.20, S 5.68. Single crystals of $2[\text{BPh}_4]_2 \cdot 2\text{MeCN} \cdot 0.5\text{H}_2\text{O}$ suitable for an X-ray structure analysis were grown by slow evaporation of an ethanol/acetonitrile solution of $2[\text{BPh}_4]_2$. These crystals slowly lose solvent molecules of solvent of crystallization at ambient temperature and turn dull.

$[\text{LNi}_2(\text{terephthalato})][\text{ClO}_4]_2$ ($3[\text{ClO}_4]_2$): Triethylamine (50 mg, 0.50 mmol) was added to a solution of terephthalic acid (41.5 mg, 0.250 mmol) in methanol (30 mL). A solution of $[\text{LNi}^{\text{II}}_2\text{Cl}][\text{ClO}_4]$ ($1[\text{ClO}_4]$) (461 mg, 0.500 mmol) in methanol (50 mL) was slowly added resulting in the immediate formation of a green precipitate. After the addition was complete, further $\text{LiClO}_4 \cdot 3\text{H}_2\text{O}$ (160 mg,

1.00 mmol) dissolved in methanol (2 mL) was added, and stirring was continued for additional 3 h. The pale-green product was collected by filtration, washed several times with cold methanol to remove any soluble impurities, and dried in the air. Yield 358 mg (74%), m.p. 317–318 °C (decomp.). IR (KBr): $\tilde{\nu}$ = 3443 (m), 2962 (s), 2868 (s), 2020 (w), 1719 (w), 1584 [s, $\nu_{\text{asym}}(\text{RCO}_2^-)$], 1463 (s), 1423 (m), 1392 [s, $\nu_{\text{sym}}(\text{RCO}_2^-)$], 1364 (m), 1309 (w), 1292 (w), 1265 (w), 1234 (m), 1201 (w), 1170 (w), 1153 (w), 1097 [ν_s , $\nu_3(\text{ClO}_4^-)$], 1060 (s), 1040 (s), 1017 (w), 1001 (w), 982 (w), 931 (m), 913 (m), 881 (m), 825 (s), 807 (m), 752 (m), 694 (w), 669 (w), 623 [s, $\nu_4(\text{ClO}_4^-)$], 601 (w), 564 (w), 538 (m), 493 (w), 446 (w), 437 (w), 417 cm^{-1} (w).

[(LNi₂)₂(terephthalato)][BPh₄]₂ (3[BPh₄]₂): A solution of NaBPh₄ (342 mg, 1.00 mmol) in ethanol (100 mL) was added to a warm solution of 3[ClO₄]₂ (194 mg, 0.100 mmol) in acetonitrile (150 mL). The reaction mixture was allowed to stir for 1 h. Upon concentration of the solution a green microcrystalline precipitate formed, which was filtered, washed with ethanol and dried in the air for 2 d yielding 214 mg (90%) of 3[BPh₄]₂ as a green powder, m.p. > 365 °C. IR (KBr): $\tilde{\nu}$ = 3436 (s), 3053 (s), 3032 (s), 3121 (w), 2962 (s), 2866 (s), 2807 (m), 1940 (w), 1879 (w), 1812 (w), 1762 (w), 1583 [s, $\nu_{\text{asym}}(\text{CO}_2^-)$], 1460 (s), 1424 (s), 1390 [s, $\nu_{\text{sym}}(\text{CO}_2^-)$], 1364 (s), 1308 (m), 1265 (m), 1233 (m), 1201 (w), 1170 (w), 1152 (m), 1112 (w), 1076 (s), 1059 (s), 1041 (s), 1001 (w), 982 (w), 929 (m), 912 (m), 882 (m), 823 (s), 734 [s, $\nu(\text{BPh}_4^-)$], 704 [s, $\nu(\text{BPh}_4^-)$], 668 (w), 629 (m), 612 (s), 563 (w), 538 (m), 491 (w), 471 (w), 416 cm^{-1} (w). UV/Vis (CH₂Cl₂): λ_{max} (ϵ) = 651 (27), 1118 nm (62 $\text{M}^{-1}\text{cm}^{-1}$). C₁₃₂H₁₇₂B₂N₁₂Ni₄O₄S₄ (2375.51): calcd. C 66.74, H 7.30, N 7.08, S 5.40; found C 66.50, H 7.16, N 7.09, S 5.66. Single crystals of 3[BPh₄]₂·2EtOH·0.5MeCN·H₂O suitable for an X-ray crystal structure analysis were grown by slow evaporation of a solution of 3[BPh₄]₂ dissolved in ethanol/acetonitrile (1:1).

[(LNi₂)₂(isophthalate)][ClO₄]₂ (4[ClO₄]₂): Triethylamine (51 mg, 0.50 mmol) and solid [LNi^{II}₂Cl][ClO₄] (I[ClO₄]) (461 mg, 0.500 mmol) was added to a solution of isophthalic acid (41.5 mg, 0.250 mmol) in MeOH (30 mL) with stirring at ambient temperature. The resulting green suspension was stirred overnight. A meth-

anol solution (5 mL) of LiClO₄·3H₂O (320 mg, 2.00 mmol) was added and stirring was continued for another 3 h. The green precipitate was filtered, washed with cold ethanol, and dried in the air. Yield 368 mg (76%), m.p. 331–332 °C (decomp.). IR (KBr): $\tilde{\nu}$ = 3426 (m), 2962 (s), 2869 (s), 1716 (w), 1607 (s) [$\nu_{\text{as}}(\text{RCO}_2^-)$], 1573 (s), 1462 (s), 1422 [m, $\nu_s(\text{RCO}_2^-)$], 1394 (s), 1364 (m), 1308 (w), 1265 (w), 1233 (w), 1202 (w), 1153 (m), 1096 [ν_s , $\nu_3(\text{ClO}_4^-)$], 1078 (s), 1041 (s), 1000 (w), 982 (w), 931 (w), 913 (w), 881 (w), 825 (m), 818 (m), 808 (w), 739 (w), 713 (w), 624 [m, $\nu_4(\text{ClO}_4^-)$], 564 (w), 540 (w), 491 (w), 463 (w), 452 (w), 428 (w), 413 (w), 405 cm^{-1} (w). UV/Vis (CH₃CN): λ_{max} (ϵ) = 265 (14869), 304 (12212), 330 (9902), 640 (49), 1141 nm (76 $\text{M}^{-1}\text{cm}^{-1}$).

[(LNi₂)₂(isophthalate)][BPh₄]₂ (4[BPh₄]₂): This salt was prepared in much the same way as described for 2[BPh₄]. To a suspension of 4[ClO₄]₂ (201 mg, 0.100 mmol) in acetonitrile (50 mL) was added a solution of NaBPh₄ (342 mg, 1.00 mmol) in ethanol (50 mL). After the resulting mixture was stirred for 2 h, the suspension was filtered, washed with ethanol, and dried in the air. Yield 225 mg (95%), m.p. 334–335 °C (decomp.). IR (KBr): $\tilde{\nu}$ = 3448 (w), 3053 (m), 3030 (m), 2962 (s), 2865 (s), 1815 (w), 1603 [s, $\nu_{\text{asym}}(\text{RCO}_2^-)$], 1564 (s), 1460 (s), 1426 [m, $\nu_{\text{sym}}(\text{RCO}_2^-)$], 1381 (s), 1307 (w), 1265 (m), 1233 (w), 1201 (w), 1152 (w), 1078 (m), 1059 (m), 1041 (m), 999 (w), 929 (w), 911 (w), 882 (w), 824 (m), 734 [s, $\nu(\text{BPh}_4^-)$], 704 [s, $\nu(\text{BPh}_4^-)$], 627 (m), 612 (m), 563 (w), 534 (w), 466 (w), 428 cm^{-1} (w). UV/Vis (CH₃CN): λ_{max} (ϵ) = 304 (13511), 330 (10913), 648 (61), 1106 nm (87 $\text{M}^{-1}\text{cm}^{-1}$). C₁₃₂H₁₇₂B₂N₁₂Ni₄O₄S₄ (2375.51): calcd. C 66.74, H 7.30, N 7.08, S 5.40; found C 65.31, H 7.36, N 6.78, S 5.31. Single crystals of 4[BPh₄]₂·4MeCN·EtOH suitable for an X-ray crystal structure analysis were grown by slow evaporation of a solution of 4[BPh₄]₂ in ethanol/acetonitrile.

Collection and Reduction of X-ray Data: Suitable single crystals of 2[BPh₄]₂·MeCN·0.5H₂O, 3[BPh₄]₂·2EtOH·MeCN_{0.5}·H₂O and 4[BPh₄]₂·4MeCN·EtOH were selected and mounted on the tip of a glass fibre using perfluoropolyether oil. The data sets were collected at 210(2) K using a Bruker SMART CCD diffractometer or a STOE IPDS-2T diffractometer. Graphite-monochromated Mo-K α radiation (λ = 0.71073 Å) was used throughout. The data were pro-

Table 2. Crystallographic data for complexes 2[BPh₄]₂·MeCN·H₂O, 3[BPh₄]₂·2EtOH·MeCN_{0.5}·H₂O, and 4[BPh₄]₂·4MeCN·EtOH.

Compound	2[BPh ₄] ₂ ·MeCN·H ₂ O	3[BPh ₄] ₂ ·2EtOH·MeCN _{0.5} ·H ₂ O	4[BPh ₄] ₂ ·4MeCN·EtOH
Formula	C ₁₃₀ H ₁₇₃ B ₂ N ₁₃ Ni ₄ O ₅ S ₄	C ₁₃₇ H _{187.5} B ₂ N _{12.5} Ni ₄ O ₇ S ₄	C ₁₄₂ H ₁₉₀ B ₂ N ₁₆ Ni ₄ O ₅ S ₄
<i>M_r</i> [g/mol]	2382.51	2506.20	2585.80
Space group	<i>P</i> $\bar{1}$	<i>P</i> $\bar{1}$	<i>P</i> $\bar{1}$
<i>a</i> [Å]	14.325(3)	15.929(3)	13.115(2)
<i>b</i> [Å]	18.128(4)	16.817(3)	17.965(2)
<i>c</i> [Å]	26.297(5)	25.687(5)	29.867(1)
α [°]	78.20(3)	97.73(3)	84.74(1)
β [°]	80.86(3)	100.44(3)	80.21(1)
γ [°]	75.11(3)	94.28(3)	76.94(1)
<i>V</i> [Å ³]	6419(2)	6671(2)	6745(1)
<i>Z</i>	2	2	2
<i>d</i> _{calcd.} [g/cm ³]	1.249	1.248	1.273
Crystal size [mm]	0.25 × 0.25 × 0.25	0.25 × 0.25 × 0.25	0.30 × 0.30 × 0.30
μ (Mo-K α) [mm ⁻¹]	0.699	0.677	0.672
2 θ limits [°]	2.36–56.64	2.46–56.64	6.38–55.96
Measured reflections	59137	61365	63201
Independent reflections	30293	31445	32119
Observed reflections ^[a]	11268	12048	22292
Number of parameters	1457	1441	1562
<i>R</i> ^[b] (<i>R</i> ₁ all data)	0.0530 (0.1657)	0.0544 (0.1596)	0.0375 (0.0644)
<i>wR</i> ₂ ^[c] (<i>wR</i> ₂ all data)	0.1386 (0.1871)	0.1368 (0.1675)	0.0782 (0.0839)
Max., min. peaks [e/Å ³]	1.777, -0.760	1.249, -0.747	0.871, -0.524

[a] Observation criterion: $I > 2\sigma(I)$. [b] $R_1 = \sum |F_o| - |F_c| / \sum |F_o|$. [c] $wR_2 = \{\sum [w(F_o^2 - F_c^2)^2] / \sum [w(F_o^2)^2]\}^{1/2}$.

cessed with the programs SAINT (2, 3)^[54] or STOE X-AREA (for 4)^[55] and corrected for absorption.^[56] Selected details of the data collection and refinement are given in Table 2. The structures were solved by direct methods^[57] and refined by full-matrix least-squares techniques on the basis of all data against F^2 using SHELXL-97.^[58] PLATON was used to search for higher symmetry.^[59] H atoms were placed at calculated positions and refined as riding atoms with isotropic displacement parameters. All non-hydrogen atoms were refined anisotropically, except for those of some disordered solvate molecules.

Some of the solvate molecules in 2, 3, and 4 were found to be severely disordered and/or only partially occupied. In the crystal structure of 2[BPh₄]₂·MeCN·H₂O one *t*Bu group and the MeCN and H₂O solvate molecules were found to be disordered over two sites. The respective orientations were refined using a split atom model to give site occupancy factors of 0.51(2)/0.49(2) (for C(32a)–C(34a) and C(32c)–C(34c)), 0.62(2)/0.38(2) (for N(7)C(41a)C(42a) and N(7)C(41b)C(42b)), and 0.78(2)/0.22(2) (for O(5a) and O(5b)), respectively. The C, N, and O atoms of the solvate molecules could only be refined isotropically, and geometric constraints using SADI instructions were required to keep the structure of the MeCN molecule reasonable. Water and acetonitrile hydrogen atoms were not included in the refinement. The solvate molecules in 3[BPh₄]₂·2EtOH·0.5MeCN·H₂O were found to be severely disordered. It was not possible to resolve this disorder, and geometric constraints using SADI instructions had to be used to maintain the structure of the solvate molecules reasonable. The occupancy factors of two EtOH and the MeCN were reduced to 0.5. The C, N, and O atoms of all solvate molecules were refined isotropically. Finally, the EtOH molecule in 4 was also found to be disordered over two sites. The disorder was refined by using a split atom model with restrained C–O and C–C distances applying SADI instructions to give site occupancies of 0.59(2) for O(3)C(54A)C(55) and 0.41(2) O(3)C(54B)C(55), respectively. Graphics were produced with Ortep3^[60] for Windows.

CCDC-654069 (for 2), -654070 (for 3), and -654071 (for 4) contain the supplementary crystallographic data for this paper. These data can be obtained free of charge from the Cambridge Crystallographic Data Centre via www.ccdc.cam.ac/data_request/cif.

Supporting Information (see also the footnote on the first page of this article): Experimental and calculated magnetic susceptibility data for all compounds.

Acknowledgments

We sincerely thank the Deutsche Forschungsgemeinschaft (DFG) (priority program 1137 “Molecular Magnetism”) for funding of this work.

- [1] F. A. Cotton, G. Wilkinson, C. A. Murillo, M. Bochmann, *Advanced Inorganic Chemistry*, 6th ed., John Wiley & Sons, Weinheim, 1999, p. 486.
- [2] a) F. A. Cotton, J. P. Donahue, C. A. Murillo, *J. Am. Chem. Soc.* **2003**, *125*, 5436–5450; b) F. A. Cotton, J. P. Donahue, C. A. Murillo, L. M. Perez, *J. Am. Chem. Soc.* **2003**, *125*, 5486–5492.
- [3] a) M. Eddaoudi, D. B. Moler, H. Li, B. Chen, T. M. Reineke, M. O’Keefe, O. M. Yaghi, *Acc. Chem. Res.* **2001**, *34*, 319–330; b) M. Eddaoudi, J. Kim, J. B. Wachter, H. K. Chae, M. O’Keefe, O. M. Yaghi, *J. Am. Chem. Soc.* **2001**, *123*, 4368–4369; c) J. L. C. Rowsell, A. R. Milward, K. S. Park, O. M. Yaghi, *J. Am. Chem. Soc.* **2004**, *126*, 5666–5667; d) T. J. Barton, L. M. Bull, W. G. Klemperer, D. A. Loy, B. McEnaney, M. Misono, P. A. Monson, G. Pez, G. W. Scherer, J. C. Vartuli, O. M. Yaghi, *Chem. Mater.* **1999**, *11*, 2633–2656.
- [4] C. N. R. Rao, S. Natarajan, A. Choudhury, S. Neeraj, A. A. Ayi, *Acc. Chem. Res.* **2001**, *34*, 80–87.
- [5] B. Moulton, M. J. Zaworotko, *Chem. Rev.* **2001**, *101*, 1629–1658.
- [6] S. Kitagawa, R. Kitaura, S. Noro, *Angew. Chem.* **2004**, *116*, 2388–2430; *Angew. Chem. Int. Ed.* **2004**, *43*, 2334–2375.
- [7] S. Kitagawa, S. Noro, T. Nakamura, *Chem. Commun.* **2006**, 701–707.
- [8] O. Kahn, *Molecular Magnetism*, VCH, Weinheim, 1993.
- [9] *Magneto-Structural Correlation in Exchange Coupled Systems* (Eds.: R. D. Willet, D. Gatteschi, O. Kahn), NATO ASI Series, Redidel, Dordrecht, 1985.
- [10] J. S. Miller, A. J. Epstein, *Angew. Chem.* **1994**, *106*, 399–432; *Angew. Chem. Int. Ed. Engl.* **1994**, *33*, 385–418.
- [11] M. Julve, J. Faus, M. Verdaguier, A. Gleizes, *J. Am. Chem. Soc.* **1984**, *106*, 8306–8308.
- [12] a) J. J. Girerd, O. Kahn, M. Verdaguier, *Inorg. Chem.* **1980**, *19*, 274–276; b) E. Bakalbassis, P. Bergerat, O. Kahn, S. Jeannin, Y. Jeannin, Y. Dromzee, M. Guillot, *Inorg. Chem.* **1992**, *31*, 625–631; c) O. Kahn, C. J. Martinez, *Science* **1998**, *279*, 44–48.
- [13] L. Deakin, A. M. Arif, J. S. Miller, *Inorg. Chem.* **1999**, *38*, 5072–5077.
- [14] P. S. Mukherjee, T. K. Maji, G. Mostafa, J. Ribas, M. S. E. Fallah, N. R. Chaudhuri, *Inorg. Chem.* **2001**, *40*, 928–931.
- [15] D. Gatteschi, R. Sessoli, A. Cornia, *Chem. Commun.* **2000**, 725–732.
- [16] D. Gatteschi, R. Sessoli, *Angew. Chem.* **2003**, *115*, 278–309; *Angew. Chem. Int. Ed.* **2003**, *42*, 268–297.
- [17] O. Sato, J. Tao, Y.-Z. Zhang, *Angew. Chem.* **2007**, *119*, 2200–2236; *Angew. Chem. Int. Ed.* **2007**, *46*, 2152–2187.
- [18] T. R. Felthouse, E. J. Laskowski, D. N. Hendrickson, *Inorg. Chem.* **1977**, *16*, 1077–1089.
- [19] a) M. Julve, M. Verdaguier, A. Gleizes, M. Philoche-Levisalles, O. Kahn, *Inorg. Chem.* **1984**, *23*, 3808–3818; b) S. Alvarez, M. Julve, M. Verdaguier, *Inorg. Chem.* **1990**, *29*, 4500–4507.
- [20] M. Verdaguier, J. Gouteron, S. Jeannin, Y. Jeannin, O. Kahn, *Inorg. Chem.* **1984**, *23*, 4291–4296.
- [21] a) E. G. Bakalbassis, C. A. Tsipis, J. Mrozinski, *Inorg. Chem.* **1985**, *24*, 4231–4233; b) E. G. Bakalbassis, J. Mrozinski, C. A. Tsipis, *Inorg. Chem.* **1986**, *25*, 3684–3690; c) C. E. Xanthopoulos, M. P. Sigalas, G. A. Katsoulos, C. A. Tsipis, A. Terzis, M. Mentzafos, A. Hountas, *Inorg. Chem.* **1993**, *32*, 5433–5436.
- [22] P. Chaudhuri, K. Oder, K. Wiegardt, S. Gehring, W. Haase, B. Nuber, J. Weiss, *J. Am. Chem. Soc.* **1988**, *110*, 3657–3658.
- [23] R. E. Coffman, G. R. Buettner, *J. Phys. Chem.* **1979**, *83*, 2387–2392.
- [24] K. S. Burger, P. Chaudhuri, K. Wiegardt, B. Nuber, *Chem. Eur. J.* **1995**, *1*, 583–589.
- [25] C. Erasmus, W. Haase, *Spectrochim. Acta, Ser. A* **1994**, *50*, 2189–2195.
- [26] J. Cano, G. De Munno, J. L. Sanz, R. Ruiz, J. Faus, F. Lloret, M. Julve, A. Caneschi, *J. Chem. Soc. Dalton Trans.* **1997**, 1915–1923.
- [27] Y. Journaux, T. Glaser, G. Steinfeld, V. Lozan, B. Kersting, *Dalton Trans.* **2006**, 1738–1748.
- [28] *Magnetism: Molecules to Materials* (Eds.: J. S. Miller, M. Drillon), Wiley-VCH, Weinheim, 2001.
- [29] E. Coronado, P. Delhaes, D. Gatteschi, J. S. Miller, Eds., *Molecular Magnetism: From Molecular Assemblies to Devices*, NATO ASI Series, Kluwer, Dordrecht, The Netherlands, 1995, vol. 321.
- [30] S. P. Watton, P. Fuhrmann, L. E. Pence, A. Caneschi, A. Cornia, G. L. Abbati, S. J. Lippard, *Angew. Chem.* **1997**, *109*, 2917–2919; *Angew. Chem. Int. Ed. Engl.* **1997**, *36*, 2774–2776.
- [31] J. Lariionova, M. Gross, M. Pilkington, H. Andres, H. Stoeckli-Evans, H. U. Güdel, S. Decurtins, *Angew. Chem.* **2000**, *112*, 1667–1672; *Angew. Chem. Int. Ed.* **2000**, *39*, 1605–1609.

- [32] A. L. Dearden, S. Parsons, R. E. P. Winpenny, *Angew. Chem.* **2001**, *113*, 155–158; *Angew. Chem. Int. Ed.* **2001**, *40*, 151–154.
- [33] S. Demeshko, G. Leibelng, S. Dechert, F. Meyer, *Dalton Trans.* **2006**, 3458–3465.
- [34] B. Kersting, G. Steinfeld, D. Siebert, *Chem. Eur. J.* **2001**, *7*, 4253–4258.
- [35] M. Gressenbuch, B. Kersting, *Eur. J. Inorg. Chem.* **2007**, 90–102.
- [36] K. Nakamoto, *Infrared and Raman Spectra of Inorganic and Coordination Compounds*, John Wiley & Sons, New York, **1986**.
- [37] F. A. Cotton, J. P. Donahue, C. Lin, C. A. Murillo, *Inorg. Chem.* **2001**, *40*, 1234–1244.
- [38] E. G. Bakalbassis, A. P. Bozopoulos, J. Mrozinski, P. J. Rentzeperis, C. A. Tipsis, *Inorg. Chem.* **1988**, *27*, 529–532.
- [39] C. S. Hong, J. H. Yoon, J. H. Lim, H. H. Ko, *Eur. J. Inorg. Chem.* **2005**, 4818–4821.
- [40] S. K. Shakhathreh, E. G. Bakalbassis, I. Bruedgam, H. Hartl, J. Mrozinski, C. A. Tspis, *Inorg. Chem.* **1991**, *30*, 2801–2806.
- [41] C. Ma, C. Chen, Q. Liu, F. Chen, D. Liao, L. Li, L. Sun, *Eur. J. Inorg. Chem.* **2004**, 3316–3325.
- [42] S. A. Bourne, J. J. Lu, A. Mondal, B. Moulton, M. J. Zaworotko, *Angew. Chem.* **2001**, *113*, 2169–2171; *Angew. Chem. Int. Ed.* **2001**, *40*, 2111–2114.
- [43] S. Bayly, J. A. McCleverty, M. D. Ward, D. Gatteschi, F. Totti, *Inorg. Chem.* **2000**, *39*, 1288–1293.
- [44] L. Li, D. Liao, Z. Jiang, S. Yan, *Inorg. Chem.* **2002**, *41*, 421–424.
- [45] Z. L. Deng, J. Shi, Z. H. Jiang, D. Z. Liao, S. P. Yan, G. L. Wang, H. G. Wang, R. J. Wang, *Polyhedron* **1992**, *11*, 885–887.
- [46] T. Beissel, T. Glaser, F. Kesting, K. Wieghardt, B. Nuber, *Inorg. Chem.* **1996**, *35*, 3936–3947.
- [47] K. K. Nanda, A. W. Addison, N. Paterson, E. Sinn, L. K. Thompson, U. Sakaguchi, *Inorg. Chem.* **1998**, *37*, 1028–1036.
- [48] J. Hausmann, M. H. Klingele, V. Lozan, G. Steinfeld, D. Siebert, Y. Journaux, J. J. Girerd, B. Kersting, *Chem. Eur. J.* **2004**, *10*, 1716–1728.
- [49] S. K. Hoffmann, W. Hilczler, J. Goslar, *Appl. Magn. Reson.* **1994**, *7*, 289–321.
- [50] V. Lozan, P. Solntsev, K. V. Domasevitch, B. Kersting, *Eur. J. Inorg. Chem.* **2007**, 3217–3226.
- [51] B. Kersting, G. Steinfeld, *Chem. Commun.* **2001**, 1376–1377.
- [52] E. Sinn, *Coord. Chem. Rev.* **1970**, *5*, 313–347.
- [53] P. W. Atkins, *Molecular Quantum Mechanics*, 2nd ed., Oxford University Press, Oxford, **1983**.
- [54] SAINT+ V6.02, Bruker AXS, Madison, WI, **1999**.
- [55] XAREA, Stoe & Cie, Darmstadt, Germany, **2001**.
- [56] SADABS, An empirical absorption correction program part of the SAINTplus NT version 5.10 package, BRUKER AXS, Madison, WI, **1998**.
- [57] G. M. Sheldrick, *Acta Crystallogr., Sect. A* **1990**, *46*, 467–473.
- [58] G. M. Sheldrick, *SHELXL-97*, Computer program for crystal structure refinement, University of Göttingen, Göttingen, Germany, **1997**.
- [59] A. L. Spek, *PLATON - A Multipurpose Crystallographic Tool*, Utrecht University, Utrecht, The Netherlands, **2000**.
- [60] L. J. Farrugia, *J. Appl. Crystallogr.* **1997**, *30*, 565.

Received: July 16, 2007

Published Online: October 1, 2007